DETERMINATION OF RESIDUAL STRESS FIELDS ON COLD-WORKED HOLES

Lucas Spirito Cunha, lucascunha@ig.com.br
Flávio Luiz de Silva Bussamra, flaviobu@ita.br
Instituto Tecnológico de Aeronáutica (ITA) ,Praça Marechal Eduardo Gomes, 50 – Vila das Acácias, São José dos Campos – SP , Brasil

Abstract. *The objective of this work is to propose a finite element for the determination of the influence of interference ratio, hardening rule and strain hardening exponent of material on the quantification of the residual stresses field generated at the process of hole cold expansion. The validation of the numerical model is done through an analytical solution selected from an extensive research of the modern techniques of analytical approach.*

Keywords: *cold work, residual stress, reverse yielding, Bauschinger.*

1. Introduction

Historically, the highest incidence of failure in aircraft has been associated with holes in connections joints. Extensive studies have been conducted in order to minimize the effects caused by stress concentration around loaded holes, resulting in some treatment processes, like cold work expansion. It consists on the radial expansion of the hole, where the resulting residuals compressive stresses minimize the effects of cyclic loadings [1],[2],[3],[4].

However, the benefits are neither considered in fatigue life predictions, nor in initiation and propagation of cracks. It happens because of the extreme difficulty in describing the behavior of the residual stresses field over time and the possible overlap of tension during cyclic loads over the life of the structure. The development of analytical tools also presents some obstacles, like the non-linearity nature of the expansion.

Considering these aspects, this work presents a finite element model for the analysis of cold work expansion in metal joints. Residual stresses are accessed. Also, the influence of the diameter of the tool, the law of strain hardening adopted and the strain hardening coefficient of the material are presented. This analysis will be performed by two-dimensional models, using the Finite Element Method, the MSC Visual NASTRAN for treatment of results and MSC Patran for construction of models.

2. Cold Work Expansion Process

The basic concept of the cold expansion process studied in this work was developed by Boeing at the end of the 60s in order to minimize the nucleation and propagation of cracks in critical holes.

In the year of 1969, FTI [2] (Fatigue Technology Inc.) created his own process of cold work expansion [5]. Over time new processes were developed. This paper is based on the process known as Split Sleeve Cold Expansion. This process is composed by a hydraulic unit where is coupled a mandrel and a lubricated sleeve. The assembly is then inserted in the hole and radial expansion occurs in the withdrawal of the mandrel when it passes through the sleeve in the hole. The sleeve is important in reducing the force applied by the hydraulic unit as well as in the protection and uniformity of the stress around the hole.

The basic objective of the process is obtained with the expansion of the hole is followed by plastic deformation, because of compressive residual stresses originated after the removal of the mandrel. This is the key point to minimize problems in fatigue from cyclic loading. However, the implementation of this process must be strictly controlled so that the benefits in fatigue are not overcome by the appearance of cracks originate by the process itself.

3. State of Art

Several techniques have been developed over time to infer more precisely the possible distribution of the residual stresses field around a cold-worked hole. Among these techniques it's possible to identify three distinct approaches: the experimental, analytical and numerical.

The experimental techniques include X-ray diffraction, neutron Diffraction by the method of cutting Sachs, photo-elasticity and optical measures of deformation. In general, precise results can be obtained by these types of measurements, as evidenced by some successful examples [6],[7],[8],[9],[10].

Many analytical solutions have been proposed. The complexity of the models used is correlated to the number of variables considered. In general, the analytical solutions assume a plane stress state with uniform radial expansion on an infinite plate or a plane strain state with uniform radial expansion of a axisymmetric cylinder [11],[12].

Hsu & Forman [13] proposed an exact solution for elastic-plastic stress in an infinite plate with hole using the law of Ramberg-Osgood modified and the criteria of Budiansky [14]. This was extended by Ball [15], [16] who added the unloading elastic-plastic and considered the presence of a zone of reverse yielding. This solution followed other reviews such as Rich & Impellizzeri [17], which considers the flow behavior during the unloading and of the Bauschinger effect proposed in Chen [18] and Zhu & Zha [19]. Recently, the consideration of the Bauschinger effect for the steady-state deformations was proposed by Wang [20] and the solution of Hsu & Forman [13] was extended by Guo [21] which took into account the effects of a plate of finite size to a plane stress state.

The numerical techniques typically employ the finite elements. Through its use is still possible to overcome obstacles not possible for analytical methodology and closer to the experimental results. The extensive use of these techniques has allowed more refined approaches making considerations such as the nonlinearity of the material, the deformation of the tool and the three-dimensional modeling for assessing the influence of thickness on the field of residual stresses.

Following there is a description of the most used analytical solutions to obtain residual stresses. The models are detailed and compared with some results taken from the article by Wang and Zhang [19].

Four analytical solutions will be addressed in this comparison. Two of them are from the consideration of a plane stress state (Hsu and Forman [13] and Ball [15]) and the other two are based in a steady-state of deformation (Rich and Impellizzeri [17] and Chang [7]).
The theoretical considerations made by each method can be viewed in the table below:

Table 1. Considerations made by the analytical methods.

Model	Yielding Criterion	Plane stress state or plane strain state	Material Behavior	Unloading
Hsu e Forman	Von Mises	Plane stress	Elastic-plastic (Ramberg-Osgood modified)	Elastic
Ball	Von Mises	Plane stress	Elastic-plastic (Ramberg-Osgood modified)	Elastic-plastic
Chang	Von Mises	plane strain	Elastic-perfectly plastic	Elastic
Rich e Impellizzeri	Von Mises	plane strain	Elastic-plastic	Elastic

The solution of Hsu and Forman [13] was developed from the extension of the theory of Nadai taking into account the effects of hardening. The main considerations are:
   • material behavior model considering modified Ramberg-Osgood;
   • flow governed by the criterion of Von Mises;
   • elastic unloading after the withdrawal of the mandrel without reversal of flow.
This was extended by the model proposed by Ball [15] that considered the elastic-plastic unloading and allowed the inclusion of a zone of reverse yielding. The Bauschinger effect has also been considered from the inclusion of a parameter β. This solution was validated by Ball and Lowry [16] from measures of X-ray diffraction on a plate of aluminum 2124-T851 with 6.35 mm thick [7].

The model for Rich-Impellizzeri [17] is a modification of the elastic-plastic solution of Sachs [20] by adding the elastic deformation of the mandrel. The unloading is considered elastic.

Regarding the adoption of the plane strain states, experimental observations indicate the presence of significant deformation along the z axis (direction of thickness), which initially weakened the use of that assumption. Moreover, most of the analysis considering this premise requires equal in magnitude (with opposite sign) between the radial and tangential components of deformation, which can only be regarded as true in the elastic regime.

As the solution proposed by Ball [15] showed good correlation with the experimental results, it will be considered in the validation of the finite element model.

4. Results of Numerical Simulation

The conditions proposed for analytical solutions developed by Ball [15] are here adopted, in order to obtain comparative results. The following Table 2 describes the characteristics of the model:

Table 2. Model Properties

Mesh properties		Mechanical properties of the material (Aluminum Plate)	
Number of nodes	3877	Module of Young	6900 daN/mm^2
Number of elements	3750	Poisson ratio	0,33
Type of elements	Quad4 (Nastran)	Yield Stress	41,4 daN/mm^2
Hole radius	3,175 mm	Hardening ratio	7
Plate dimensions	127x127 mm		
Plate Thickness	1mm		

To simulate the different levels of interference from the mandrel and its contact with the surface of the hole, it was adopted a uniform loading along the edge of the hole, simulating the pressure in the region caused by the introduction of the tool.

For a given applied pressure on the border of the hole, the tangential strain can be found by:

$$\varepsilon_\theta = \frac{1}{E}\left[\left(\frac{\sigma}{\sigma_y}\right)^{n-1}\sigma_\theta - \left(\frac{R}{1+R}\left(\left(\frac{\sigma}{\sigma_y}\right)^{n-1}-1\right)+v\right)\sigma_r\right]$$ (1)

where E is the Young's Modulus, σ_θ and ε_θ are tangential stress and strain, respectively, σ_r is radial stress, σ_y is the yield stress, and n is the Ramberg-Osgood hardening parameter [10].

The radial displacement of the plate is given by:

$$u_p\left(a_p\right)= a_p.\varepsilon_\theta$$ (2)

The ratio of interference is calculated by:

$$I_0 = \frac{a_i - a_p}{a_p}$$ (3)

where:

$$a_p = 3.175mm$$

$$a_i = \frac{a_p + u_p\left(a_p\right)}{1-\frac{p}{E_i}\left(1-v_i\right)}$$ (4)

In order to simulate the pressure applied by the mandrel it was defined a cylindrical coordinate system on the center of the hole and it was applied on the border nodes a radial force given by:

$$F = \frac{P.2\pi.r.t}{n}$$ (5)

where P is the pressure obtained by a specified interference rate, r is the hole radius, t is the plate thickness and n is the number of nodes on hole boundary.

Finally, the orientation of the material of the plate in the direction of the radial coordinate is the same direction used in the application of nodal forces, as showed in Fig. 1.
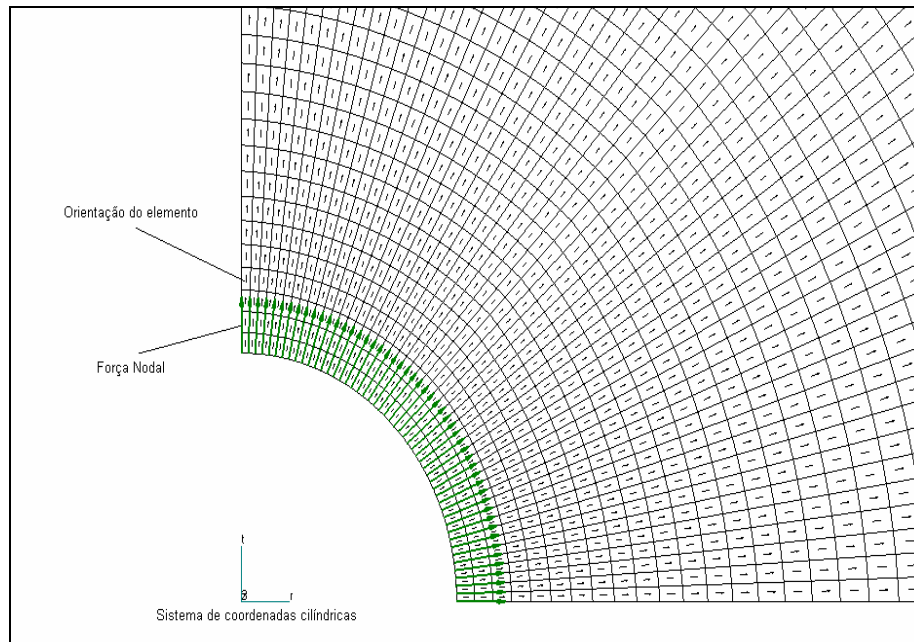
Figure 1. Material orientation and load application.

In order to simulate a condition of subsequent loading and unloading, two cases of loads were analyzed in NASTRAN. The first case presents the load conditions for the desired level of interference. The second case presents zero load in order to simulate the unloading. At this point it is necessary to state that the conditions for isotropic and kinematic strain hardening have great influence on the final result and so both were analyzed separately.

Tests were performed to analyze the convergence of the nonlinear model and some cases presented divergent solutions to the default conditions of the program.

In order to improve convergence, the default solution of the program considers a multiple criteria where the errors are measured in terms of load functions (default = 10^{-3}) and energy (default = 10^{-7}). For each increment of load the program automatically selects the most efficient strategy based on the rates of convergence. The number of iterations required for convergence is estimated and the stiffness matrix is updated if:

- the estimated number of iterations for convergence exceeds the fixed maximum number of interactions (default = 25);
- the solution diverges.

Convergence comes to an end if, for each increment of load, the error functions have less value than the established or the maximum limit of divergence (= standard condition 3) is reached.

As the default condition showed divergence for some cases, Newton-Raphson method is used, which consists of updating the stiffness matrix in each iteration. This procedure has higher computational costs, but all models tested achieved the final convergence.

4.1. Analysis results using isotropic strain hardening law

Figure 2 illustrates the results obtained. It can be seen that increasing the degree of interference causes the increase of compressive tangential residual stress at the border of the hole. Comparing the curves of residual stress tangential to the ratios of interference of 2% and 7%, the increase of compressive stress on the border of the hole is approximately 40%. The radial residual stresses show the same trend as the increasing rate of interference, but their values parameterized in terms of yielding stress are negligible in intensity compared to the tangential boundary values. But the field of residual compressive radial stress is more extensive than the tangential field and tends to surpass it in intensity as the increase of the border distance.
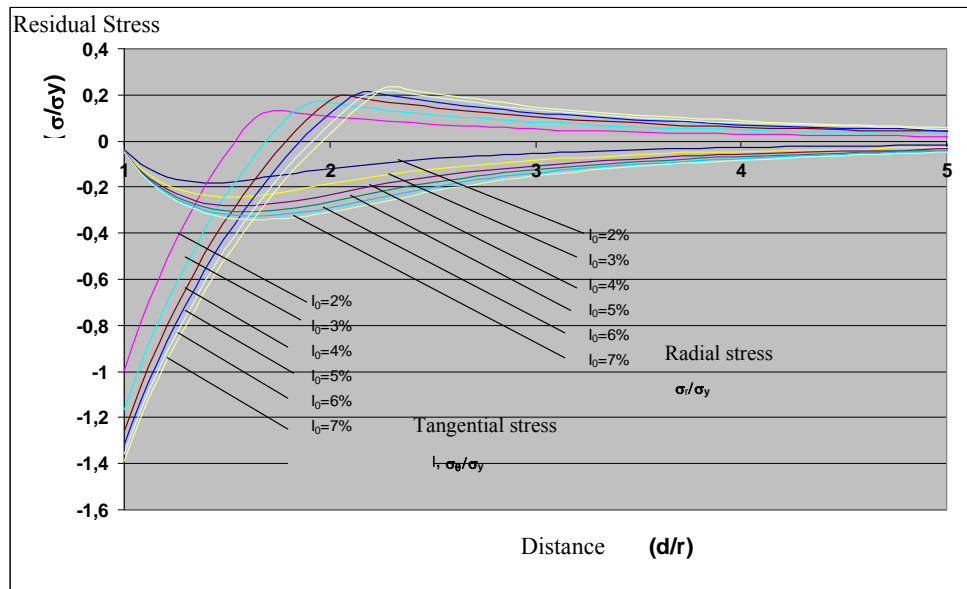

Figure 2. Distribution of tangencial and radial residual stresses in accordance with the interference rate obtained with the Nastran for isotropic hardening.

4.2. Analysis results using kinematics strain hardening law.

Looking at the Fig. 3 that illustrates the results obtained, it can be noticed that, different from the strain hardening isotropic, the intensity of tangential compressive residual stress tends to be smaller with increasing rate of interference at the border of the hole. This is due to reverse yielding, which can not be obtained when using a model with isotropic hardening.

It is also noticed that with the distance increase from the border, the tangential compressive residual stresses tend to increase until the limit of the zone of reverse yielding. The maximum intensity, however is almost equal for all levels of interference observed in the graph. We find in fact that the higher rates of interference tend to generate a field of tangential compressive residual stresses more extensive, however the maximum intensity does not differ much.

The radial residual stresses show similar behavior as the tangential ones at the border of the hole, but with the increase of distance from the hole the curves generated by higher levels of interference tend to achieve a greater maximum compressive value. For the interference rates of 2% and 7%, the difference between the maximum radial compressive stress is approximately 8%.
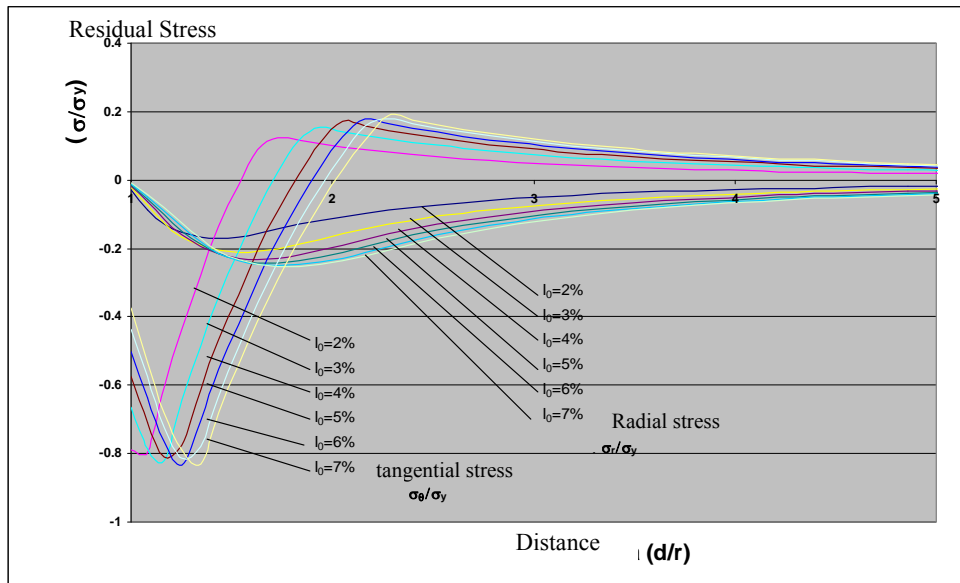
Figura 3. Distribution of tangential and radial residual stresses in accordance with the interference rate obtained with the Nastran for kinematics hardening.

Figure 4 below compares the curve of tangential residual stress to interference rate of 4% with the stress distribution provided by the program of finite elements in order to identify the zone of reverse yielding, the main factor that differentiates the isotropic analysis from the kinematics. Figure 6 presents the behavior obtained in the analysis considering isotropic hardening law and Fig. 7 presents the behavior obtained in the analysis considering the kinematic hardening.
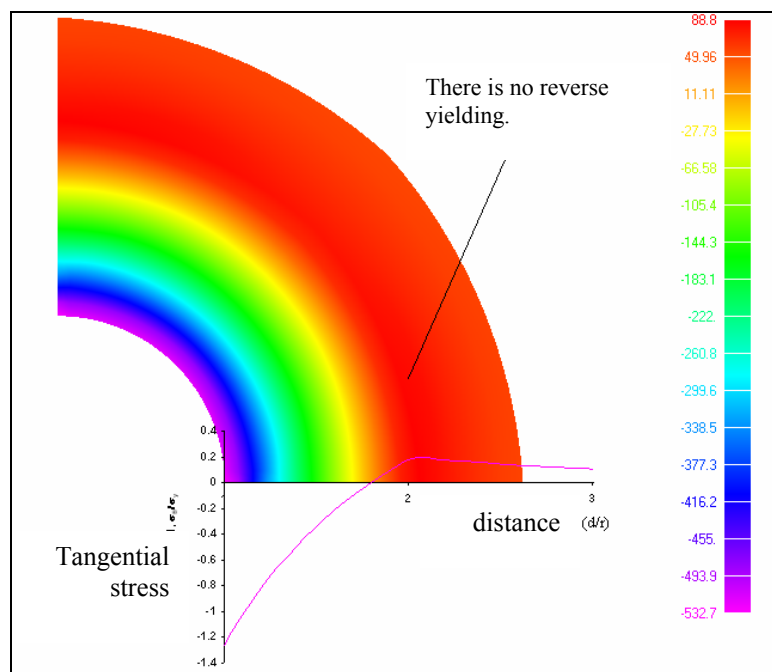

Figure 4. Representation of the tangential residual stress distribution and identification of the yielding zone considering isotropic hardening and interference rate of 4%.
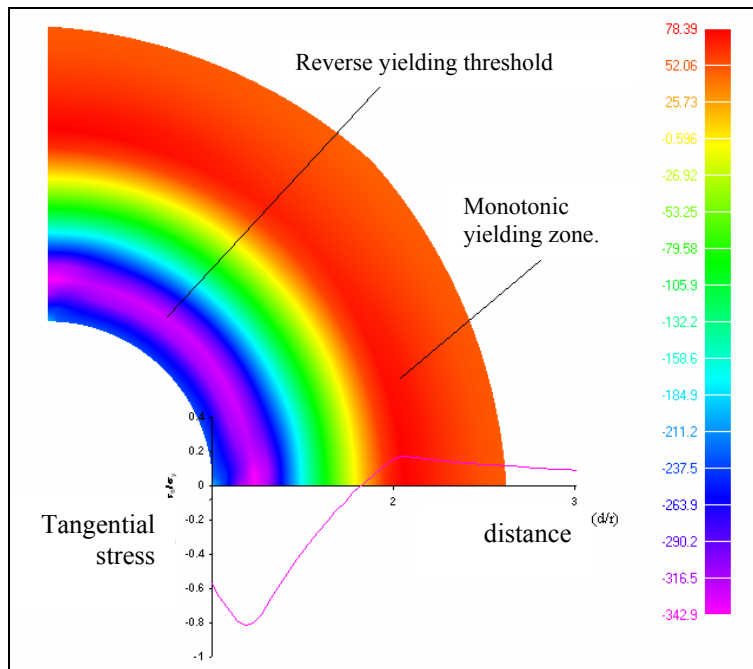
Figure 5. Representation of the tangential residual stress distribution and identification of the yielding zone considering kinematics hardening and interference rate of 4%.

4.3. Results of analysis for the variation of the hardening coefficient of the material

Looking at the Fig. 6 that illustrates the results obtained, one can notice that material with higher degree of strain hardening(n less) tend to have the field of compressive residual stresses lower in intensity and extent for both tangential and radial components.
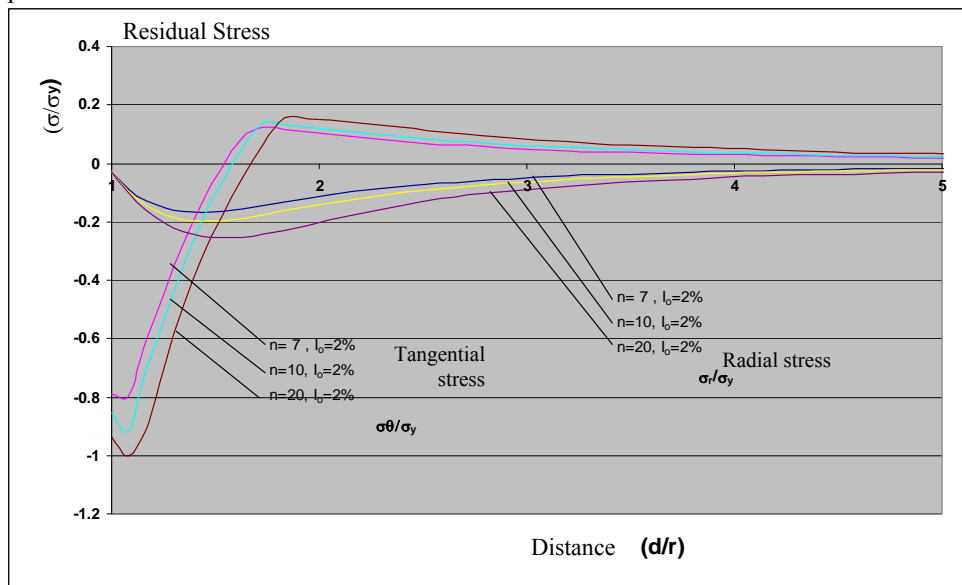

Figure 6. Distribution of tangential and radial residual stresses in accordance with the hardening coefficient.

4.4. Comparison between numerical and analytical results

For an interference ratio of 4%, Fig. 7 summarizes the results provided by numerical tool and the analytical solution based on both the isotropic and the kinematic hardening. The analytical points were obtained by creating an analytical tool using the formulas created by Ball [12].
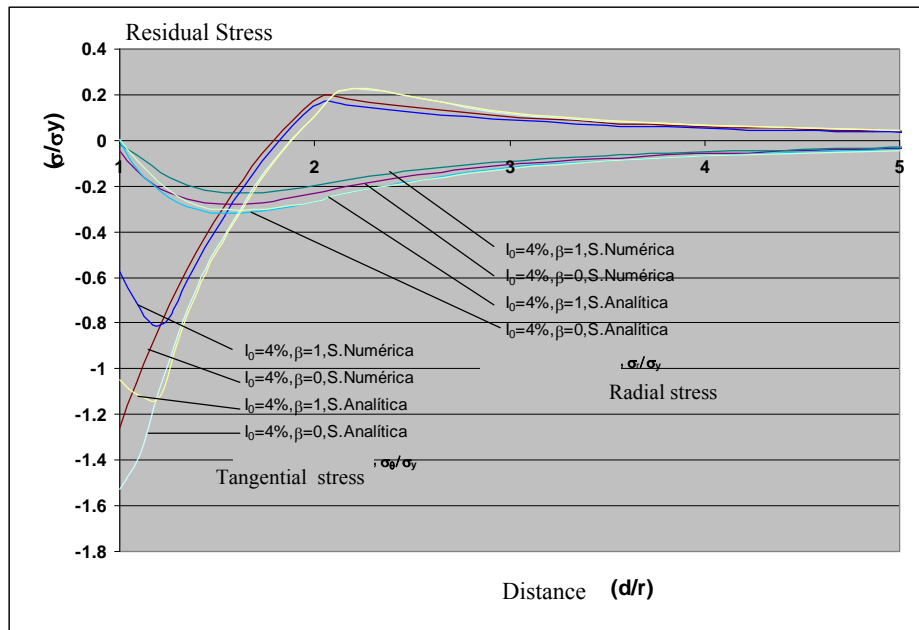
Figure 7. Comparison between the tangential and residual distribution obtained by analytical and numerical methodology.

Regarding the compressive tangential residual stresses it was observed that the analytical results for both isotropic and kinematics strain hardening present higher intensities than the numerical results. On the borderline of the hole this difference is more pronounced in kinematics hardening, reaching the value of 45.15%. However with the increase of distance from the hole borderline, this difference drops to about 25% despite the law adopted for the material. The difference increases again when the curves are closer of the tension behavior, reaching 69% for isotropic hardening and 45% for kinematics hardening. After the point of inflection, where stresses tend to zero, percentage differences decrease as expected.

Regarding the radial residual stresses it was also observed an increased intensity in the analytical results compared to numerical results with few exceptions. On the borderline of the hole as the stresses are low, the percentage difference is very high, but after a short distance it was observed difference with almost constant values reaching approximately 25% to kinematics hardening and 12% for isotropic hardening.

Despite the differences, the curves resulting from numerical and analytical analysis show similar behaviors.

5. Conclusions

An extensive literature review was carried out to identify the main analytical solutions for the determination of residual stresses at cold worked holes. At this point it was identified the solution proposed by Ball [15] as the most effective and closer to the experimental values available at literature.

The analytical solution was used as a comparative basis for the proposed finite element model. It was created an efficient mesh, seeking the convergence of the model against the non-linear analysis and minimization of computational time. Some critical parameters were varied in order to assess its influence on the distribution of the residual stresses.

The conclusions regarding these parameters are:

• β (the Bauschinger parameter): this parameter was evaluated in the finite element model through variation of the hardening law. To isotropic hardening, equivalent to β=0, it was obtained higher values for maximum compressive tangential stress and increased of the same at the borderline of the hole associated to the increase of the interference ratio. For the kinematic hardening, it was observed a decrease in the maximum compressive tangential stress in the hole boundary with subsequent increase due to the zone of reverse yielding. Regarding the radial residual stress, the change was not significant.

• n – hardening coefficient of the material: this parameter was evaluated through the variation of stress-strain curve obtained from the Ramberg-Osgood modified model. It was noticed that the compressive residual stress tends to be lower for materials with low n, ie for materials with higher hardening during plastic deformation.

• I∘- rate of interference: this parameter indicates the ratio between the diameter of the hole and the diameter of the mandrel. This rate was represented in the model of finite elements through the magnitude of loads applied at the border of the hole. It was noticed that for isotropic hardening law there is an increase in maximum compressive tangential tension on the border of the hole with the increase of the rate of interference. Considering the law kinematic hardening law, it was observed that at the edge of the hole the tangential compressive stress tends to be higher for lower rates of interference, however the maximum compressive tangential stress varies slightly as increased rates of interference (in the order of 4%) and the area of reverse yielding tends to increase its width.

Regarding the comparison of results obtained analytically and numerically, there was considerable discrepancy in the values for maximum compressive tangential residual stress that varies more than 40%. However the curves showed similar behavior with occasional differences in measured values. The analytical methodology used was validated in Ball [15] by comparison with experimental results also showed differences mainly in the region near the border. So the differences between the analytical model and numerical results are reasonable considering the existent results at literature.

Looking at the overall results obtained, we can infer that the model with isotropic hardening should not be used as the reverse yielding has an important role on the determination of the compressive residual stresses on the border of the hole. The non consideration of this effect may lead to results not conservative for fatigue analysis in part because the maximum compressive residual stress on the border of the hole tends to be overestimated. Therefore the kinematic analysis tends to secure results closer to reality. Another important factor is the rate of interference of the mandrel, that looked from the point of view of the model with isotropic hardening could lead to the false impression that the increase of the same could generate higher compressive residual stresses on the border of the hole, which in reality does not occur when reverse yielding is taken in account. Indeed we observed that in kinematics hardening analysis the variation in the rate of interference does not present a great influence on the maximum compressive tangential residual stress, being important only in increasing the length of the field of compressive residua stress.

We suggest as future trends numerical analyses in three-dimensional models to determine the influence of the thickness of the plate in the behavior of the residual stresses associated with experimental testing to validate the results. We also suggest carrying out tests to check the variation of residual stress obtained over time when subjected to cyclic loadings.

6. REFERÊNCIAS

[1] Cunha, Lucas Spirito. Determinação da Distribuição de Tensão Residual ao Redor de Furos Expandidos a Frio. Master's Thesis, São José dos Campos, 2005, 90f.
[2] FTI Extending fatigue life of metal structures materials testing, Fatigue Technology Inc., 1991.
[3] Cook R, Holdway P. Residual stresses induced by hole cold expansion. In: Computer methods and experimental measurement for surface treatment effects. Great Britain: Computational Mechanics Publications; 1993. p.90-100.
[4] Chang JB. Prediction of fatigue crack growth at cold-worked fastener holes. J Aircraft 1977;14:903-8
[5] Ball DL, Lowry DR. Experimental investigation on the effects of cold expansion of fastener holes. Fatigue Fract Eng Mater Struct 1998; 21:17-34.
[6] Su X, Gu M, Yan M. A simplified residual stress model for predicting fatigue crack growth behavior at cold worked fastener holes. Fatigue Fract Eng Mater Struct 1986;9:57-64.
[7] Sharpe WN. Residual strains around coldworked fastener holes. J Eng Mater Tech 1978;100:310-312
[8] A. Nadai, Theory of Flow and Fracture of Solids, McGraw-Hill, New York, 1950.
[9] Hill, R., The Mathematical Theory of Plasticity, Oxford University Press, Oxford, 1950, pp.106-114.
[10] Hsu YC, Forman RG, Elastic-plastic analysis of an infinite sheet having a circular hole under pressure. Trans ASME, J Appl Mech 1975;42:347-52
[11] B. Budiansky (1971) An exact Solution to an elastic-plastic stress concentration problem. Prikladnaya Matematika I Physik 35, (1), 40-48
[12] Ball DL. Elastic-plastic stress analysis of cold expanded fastener holes. Fatigue Fract Eng Mater Struct 1995; 18:47-63
[13] Ball DL, Lowry DR. Experimental investigation on the effects of cold expansion of fastener holes. Fatigue Fract Eng Mater Struct 1998;21:17-34
[14] Rich DL, Impellizzeri LF. Fatigue analysis of cold-worked and interference fit fastener holes. In: Cyclic stress-strain and plastic deformation aspect of fatigue crack growth. ASTM STP 637. American Society for Testing and Materials; 1997. p.153-75.
[15] Chen, P.C.T. A new method of predicting residual stresses in autofrettaged gun barrels. ARCCB-TR-86012, US Army Armament Research and Development Center, Watervliet, 1986.

[16] Zhu, Wu-Xue, Zhai, Zi-Chu. Na elastic-plastic analysis of autofrettaged thick-walled cylinders. Acta Mechanica Sinica, 1987, 19, pp.245-255

[17] Wang, G.S. An elastic-plastic solution for a normally loaded center hole in a finite element circular body. International Journal of Pressure Vessel and Piping, 33,1988,pp.269-284.

[18] Guo, Wanlin. Elastic-plastic analysis of a finite sheet with a cold worked hole. Engineering Fracture Mechanics, 46,1993,pp.465-472.

[19] Z. Wang, X. Zhang. Predicting fatigue crack growth life for cold-worked holes base don existing closed-form residual stress models.International Journal of Fatigue, 2003.

[20] Hoffman O, Sachs G. In: Introduction to the theory of plasticity for engineers. New York: McGraw-Hill; 1953. p.80-95.